Higher power output in thermoelectric generator integrated with phase change material and metal foams under transient boundary condition

Yousefi, Esmaeil; Abbas Nejad, Ali; Rezaniakolaei, Alireza

Published in:
Energy

DOI (link to publication from Publisher):
10.1016/j.energy.2022.124644

Publication date:
2022

Document Version
Publisher's PDF, also known as Version of record

Energy 256 (2022) 124644

Contents lists available at ScienceDirect

Energy

journal homepage: www.elsevier.com/locate/energy

Higher power output in thermoelectric generator integrated with phase change material and metal foams under transient boundary condition

Esmaeil Yousefi [a], Ali Abbas Nejad [a, **], Alireza Rezania [b, *]

[a] Faculty of Mechanical Engineering, Shahrood University of Technology, Shahrood, Iran
[b] AAU Energy, Aalborg University, Pontoppidanstræde 111, Aalborg, DK-9220, Denmark

ARTICLE INFO

Article history:
Received 11 February 2022
Received in revised form
17 May 2022
Accepted 23 June 2022
Available online 30 June 2022

Keywords:
Thermoelectric generator
Transient heat source
Phase change material
Metal foams
Energy storage

ABSTRACT

Phase change materials (PCMs) are useful means for energy storage and thermal management of thermoelectric generators (TEG) systems. Nevertheless, energy storage rate under transient heat loads is slow due to low thermal conductivity of PCMs. In this study, copper and nickel porous metal foams are applied in a PCM on hot side of a TEG to accelerate storage of fusion heat and power output of the TEG under transient boundary conditions. Therefore, continuous and fluctuating heat flows were imposed to the system initiating from ambient room temperature. Results of this study show that, adding the metal foams enhances heat flux through the PCM by reducing overall thermal resistance in the energy storage box. The PCM with copper foam makes higher percentage of increase of temperature in the box and higher power generation until the melting point, while the PCM with nickel provides higher storage temperature after the melting process. The metal foams improve the thermal conductance between the heat source and the TEG creating higher temperature difference across the module and making higher electrical power compared to the case with PCM-only. The corresponding power enhancement is 26.2% and 62.5% by the TEGs with the nickel and copper foams, respectively.

1. Introduction

The widespread consumption of fossil fuels by humans has created many environmental issues, such as ozone depletion, release of toxic gases, and destruction of ecosystems. Thermoelectric generator (TEG) is one of the effectual technologies, by recovering waste heat and converting into useful electrical energy [1,2]. TEGs are solid state devices that directly convert thermal energy into electricity. Although these devices are less efficient than the conventional heat engines, TEGs are highly applicable and have many advantages due to their small sizes and less complexity [3,4]. Thermoelectric based systems can be simple, lightweight, affordable, and without moving parts and mechanical vibration during operating. While TEGs are efficient at higher temperatures, these devices need protection from overheating and damaging at temperatures out of their operating range [5,6]. Protection of TEG modules under unstable temperature boundary conditions as well as producing appropriate power can be achieved by proper thermal management at its cold side [7,8], hot side [9] and regulation of the electrical load resistance over the TEG module [10].

Applying phase change materials (PCMs), alternatively, helps to control the hot side temperature of TEGs by absorbing a fraction of the thermal energy imposed from the heat source. Under transient heat loads, the temperature fluctuation reduces while the PCM stores thermal energy via phase changing from solid to liquid [11,12]. These materials can stabilize temperature on both sides of the TEG [13,14]. To improve thermoelectric conversion performance and to protect the module during long-term use, Meng et al. [15] developed a thermoelectric system combined with PCM. They applied the PCM on the hot, cold and both sides of the TEG under unstable heat loads, and investigated the heat transfer mechanism in the system. The results confirmed high-potential of the PCM in thermal energy storage and protection of the TEG from overheating under variable thermal loads. Wang et al. [16], furthermore, proposed a hybrid TEG-PCM system, where they showed the time to produce electricity was longer when the PCM was applied under

* Corresponding author.
** Corresponding author.
E-mail addresses: abbasnejad@shahroodut.ac.ir (A.A. Nejad), alr@energy.aau.dk (A. Rezania).

https://doi.org/10.1016/j.energy.2022.124644

Nomenclature

C_p	specific heat capacity ($Jkg^{-1}K^{-1}$)
C_{th}	equivalent thermal capacitance (JK^{-1})
R_{in}	internal resistance (Ω)
R_L	external load (Ω)
R_{th}	thermal resistance (KW^{-1})
k	thermal conductivity ($W\ m^{-1}K^{-1}$)
L	latent heat capacity (Jkg^{-1})
V	voltage (V)
T	temperature ($^{\circ}C$, K)
Q	heat transfer rate (W)
I	current (A)
ε	porosity
α	Seebeck coefficient (VK^{-1})
ρ	density ($kg\ m^{-3}$)
f	volume fraction
ΔT	temperature range over which the PCM melts (K)
h	height (m)
w	width (m)
l	length (m)
t	time (s)

Subscripts

s	solid
l	liquid
m	melting
h	hot
c	cold
pm	porous medium
eff	effective

pulsed thermal boundary conditions. They used the PCM to stabilize the hot side temperature of the TEG and to control the thermal fluctuations during energy production.

To recover dissipating heat emitted from internal combustion engines using TEGs, Mirko et al. [17] embedded PCM between hot side of the TEGs and the exhaust pipe for storing thermal energy and protecting the modules under transient thermal loads. Their results verified high potential of PCMs as an effective energy storage technology in TEG systems. In an experimental study, Jaworski et al. [18] showed possibility of using PCM as a heat sink to stabilize cold side temperature of a TEG module. In their study, the TEG system was designed as absorber of solar irradiation. In order to maximize utilization of thermal energy harvesting, Ahmadi et al. [19] suggested two-stage TEG system design using PCM, where thermal energy was stored in a PCM box and then distributed among TEGs mounted around the box. Their proposed system generated more electrical power than a one-stage TEG system with the same thermal energy input. Moreover, they used PCM for protection and thermal management of TEGs [20] by applying the PCM at hot side of the TEG, which significantly mitigated effect of temperature fluctuation of the heat source on the TEG's hot side.

PCMs have different melting temperatures, heat of fusions, and different thermal conductivities, which are important design factors in a thermal management system using PCMs. Darkwa et al. [21] investigated conversion efficiency improvement of silicon crystal photovoltaic cell with PCM and TEG at its cold side emphasizing importance of thermal conductivity of PCMs. PCMs have some substantial advantages such as high latent heat, low vapor pressure, non-toxicity, and are stable and inexpensive. On the other hand, low thermal conductivity of PCMs has limited their application in thermal systems and industries using heat. Amplification of PCM thermal conductivity makes it more efficient in controlling of the module hot side temperature and fluctuation stabilization of its output voltage [22].

Porous metal foams have been used to increase heat transfer in PCMs and for temperature stabilization under transient boundary conditions via improving thermo-physical properties of the PCMs. As results, electrical power outputs increased, and heat loss from the systems reduced [23–25]. Because of light-weight, high surface-area density and compact size, open cell metal foams have been used in vast industrial applications such as heat exchangers, high-temperature filters, solar collectors, armor sectors and medical fields [26]. To investigate transient thermal storage properties of a double pipe heat exchanger with a highly porous metal foam and PCM (paraffin RT50), Chen et al. [27] developed a dynamic heat transfer model using enthalpy-porosity method. They found reduction of the PCM melting time and significant increment in heat storage rate as effects of using the metal foam. Remarkable effects of applying metal foam to enhance heat transfer in PCMs was numerically reported by Borhani et al. [28] where they studied adding copper foam as a porous medium in low melting temperature paraffin. They evaluated effects of different porosities on a TEG performance and found that, reducing the porosity improves the TEG's conversion efficiency.

Duan [29] investigated performance of concentrated photovoltaic panel integrated with PCM and porous metal foam. His numerical study shows that, such hybrid system enhanced cooling over the photovoltaic module and its conversion efficiency significantly compared to the case where only PCM was used for the thermal management. Nithy et al. [30] investigated heat recovery from cars exhaust pipe consisted of TEG and metallic foam in a heat exchanger to reduce thermal resistance between the heat source and TEG. Madroga [31] presented a model for absorbing thermal fluctuations in a fuselage during flights with metal foam, water as PCM, and TEG as energy harvester. Although the PCM applied in his study could be used in a limited range of temperature, it was observed that, the metal foam was the main factor for enhancing conductivity and achieving higher temperature difference across the TEG. Moreover, shortening of PCM melting time and the uniformity of heat distribution during the phase change in paraffin with aluminum foam were reported by Diani et al. [32] by highlighting coupled effect of the linear porosity of the foams and the PCM melting point.

Results of our previous work [20] indicated, although using PCM on the hot side provides continuous and smother voltage generation by the TEG, thermal properties of the PCM module needs enhancement in advanced heat conduction mechanism. A PCM box with low thermal conductivity decelerates absorption of the heat and is a reason to heat transfer shortcut between the heat source and TEG via the box walls. This study, nevertheless, examines enhancement of thermal conductivity between the heat source and TEG using different metal foams inside PCM placed between them. This work investigates, in detail and experimentally, impact of metal foams on improvement of overall thermal conductivity of PCM and increment of heat transfer between the heat source and TEG under transient thermal boundary conditions. Therefore, this study aims to explore alteration of energy storage rate in the PCM and power generation by the TEG. Via focusing on the melting process and analyzing of the temperature variation on both sides of the TEG, power generation and electrical energy production under

unstable thermal boundary conditions will be explained.

The present work considers open porous copper and nickel foams with different thermal conductivities but equal volumes and specific physical characteristics in an aluminum PCM box with thin walls. Hence, three PCM modules consisting of only PCM, PCM with copper foam, and PCM with nickel foam, namely PCM-only, PCM-Cu, and PCM-Ni are investigated in this study. Equivalent RC network of the system, consisting of geometry and thermal properties of the foams and the PCM, is presented to evaluate acceleration of heat transfer and enhancement of latent heat storage under continues and fluctuating heat fluxes from the heat source. Temperature variations of the heat source, inside the PCM box, and on both sides of the TEG are measured to investigation performance of the improved system. To explain the hybrid high-heat flux and high-heat storage mechanism under transient heat sources, design concept and relevant mathematical correlations are presented in the next section. Sections 3 and 4 describe the experimental setup and test procedure, respectively followed by the results section.

2. Concept equivalent RC network and mathematical correlations

This study investigates enhancement of energy conversion performance in TEG systems integrated with energy storage modules under unstable thermal boundary conditions. This progress took place using porous metal foams and improving energy storage rate to provide proper temperature on TEG's surfaces. For this investigation, copper and nickel foams were selected. Although nickel has lower thermal conductivity than copper, it has a higher resistivity against oxidization, which makes this metal foam suitable for energy storage applications. Under thermally transient conditions, the metal foams enhance the latent-heat energy storage [33], where this study shows how higher heat of fusion can be transferred by the metal foams. To explain the heat transfer mechanism and formulation of the foams effect on the latent heat storage in the proposed thermoelectric system, the RC network model and the governing equations are presented. The RC network model of the studied TEG system is shown in Fig. 1. The terms of R and C represent the thermal resistance and heat capacitance, respectively. During the phase changing stage, a large amount of thermal energy is stored; so that the PCM can be considered as a large thermal capacitor [34]. The heat transfer across the box walls, the PCM and foams are included in the RC network.

R and C can be calculated by Eqs. (1) and (2) where h, w, and l are the thickness, width and length of the elements, respectively [35]:

$$R_{th} = \frac{h}{w.l.k} \tag{1}$$

$$C_{th} = h.w.l.\rho.C_{app} \tag{2}$$

In Eq. (3), C_{app} is the apparent heat capacity of the PCM defined as:

$$C_{app} = \begin{cases} C_p \quad , \quad T \le T_{melt} \\ C_p + \dfrac{L}{\Delta T} \ , \ T_{melt} < T < T_{melt} + \Delta T \\ C_p \quad , \quad T \ge T_{melt} + \Delta T \end{cases} \tag{3}$$

where the temperature range over which the PCM melts is the ΔT. The equivalent heat resistance and heat capacitance of the PCM-only system from A to B in Fig. 1 can be calculated as follow:

$$\frac{1}{R_{th,AB}} = \frac{1}{R_{Al}} + \frac{1}{R_{PCM}} \tag{4}$$

$$R_{th,AB} = \frac{R_{Al}R_{PCM}}{R_{PCM} + R_{Al}} \tag{5}$$

$$C_{th,AB} = C_{th,Al} + C_{th,PCM} \tag{6}$$

In these equations, R_{Al} and $C_{th,Al}$ between A and B represent the thermal resistance and heat capacitance of the aluminum box walls. After adding the foams, Eqs. (5) and (6) change as follow:

$$\frac{1}{R_{th,AB}} = \frac{1}{R_{Al}} + \frac{1}{R_{PCM}} + \frac{1}{R_{Foam}} \tag{7}$$

$$C_{th,AB} = C_{th,Al} + C_{th,PCM} + C_{th,Foam} \tag{8}$$

Therefore, the equivalent resistance inside the box (A to B)

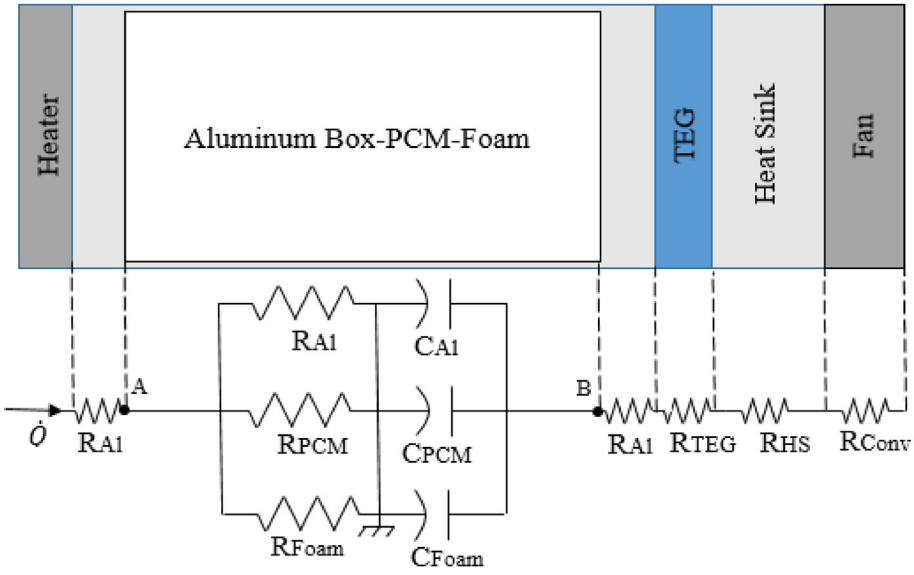

Fig. 1. RC network model of the TEG system including PCM and metal foam.

decreases with adding the foam while the heat capacitance increases. With following substitutions made in Eqs. (7) and (8):

$$\frac{1}{R_{pm}} = \frac{1}{R_{PCM}} + \frac{1}{R_{Foam}} \tag{9}$$

$$C_{th,pm} = C_{th,PCM} + C_{th,Foam} \tag{10}$$

$R_{th,AB}$ and $C_{th,AB}$ in Eqs. (7) and (8) can be calculated in the aluminum box consisting of the metal foams and PCM:

$$R_{th,AB} = \frac{R_{Al}R_{pm}}{R_{pm} + R_{Al}} \tag{11}$$

$$C_{th,AB} = C_{th,Al} + C_{th,pm} \tag{12}$$

where thermal resistance and heat capacitance of porous medium are defined as:

$$R_{pm} = \frac{h}{w.l.k_{eff}} \tag{13}$$

$$C_{th,pm} = h.w.l.\overline{\rho C} \tag{14}$$

In the thermal resistance equation, Eq. (13), the term of k_{eff} is the effective conductivity of the porous medium that can be expressed as [36]:

$$k_{eff} = (1-\varepsilon)k_m + \varepsilon k_{PCM} \tag{15}$$

where k_{PCM}, the PCM conductivity, is defined as:

$$k_{PCM} = f_l k_l + (1-f_l)k_s \tag{16}$$

Meanwhile, $\overline{\rho C}$ in the Eq. (17) refers to the mean thermal capacitance of the porous medium defined as [37]:

$$\overline{\rho C} = f_l \varepsilon \rho C_l + (1-f_l)\varepsilon \rho C_s + (1-\varepsilon)\rho_m C_m \tag{17}$$

where ε is the porosity of the porous matrix, and C_s and C_l are the specific heat of the solid and liquid phases of the PCM, respectively. C_m shows the specific heat of the foam material, and ρ and ρ_m are the density of the PCM and porous matrix, respectively. Moreover, f_l is the volume fraction of the PCM in the liquid phase defined by Eq. (18) [38]:

$$f_l = \begin{cases} 0 \quad , T \le T_s \\ 1 \quad , T \ge T_l \\ \dfrac{T - T_s}{T_l - T_s}, \ T_s < T < T_l \end{cases} \tag{18}$$

The energy balance equations in the TEG are as follow [39]:

$$Q_h = \alpha T_h I_{TEG} + k_{in}(T_h - T_c) - 0.5R_{in}I_{TEG}^2 \tag{19}$$

$$Q_c = \alpha T_c I_{TEG} + k_{in}(T_h - T_c) + 0.5R_{in}I_{TEG}^2 \tag{20}$$

where Q_h and Q_c are heat transfer rate from both sides of the TEG and α is the Seebeck coefficient of the TEG semiconductor materials. R_{in} and k_{in} are internal resistance and thermal conductivity of the TEG, respectively. Moreover, T_h and T_c are the temperatures on the hot and cold junctions of the TEG, respectively.

The output power of the TEG can therefore be [40]:

$$P = Q_h - Q_c = \alpha I_{TEG}(T_h - T_C) - I_{TEG}^2 R_{in} \tag{21}$$

Moreover, the output power under the external electrical load and corresponding voltage across the load resistor are:

$$P = VI_{TEG} = I_{TEG}^2 R_L \tag{22}$$

$$V = I_{TEG}R_L = \alpha(T_h - T_C) - I_{TEG}R_{in} \tag{23}$$

The electric current of the module, I_{TEG}, can be calculated as:

$$I_{TEG}^2 R_L = \alpha I_{TEG}(T_h - T_C) - I_{TEG}^2 R_{in} \tag{24}$$

$$I_{TEG} = \frac{\alpha(T_h - T_c)}{R_L + R_{in}} \tag{25}$$

Furthermore, the output power of the TEG in Eq. (22) can be expressed as:

$$P = \left[\frac{\alpha(T_h - T_c)}{R_L + R_{in}}\right]^2 R_L \tag{26}$$

If $R_{in} = R_L$, the output power of the module is maximized as [41]:

$$P_{max} = \left[\frac{\alpha(T_h - T_c)}{2R_{in}}\right]^2 R_{in} = \frac{\alpha^2(T_h - T_c)^2}{4R_{in}} \tag{27}$$

3. Experimental setup and theoretical calculations

Fig. 2A shows the setup components investigated in this study. In this system, two ceramic heat plates with maximum voltage and power of 220 V and 210 W, respectively, and dimensions of 15 $mm\times$ 70 $mm\times$ 1.5 mm were used to simulate the heat loads. A TEG module (Bismuth Telluride, SP1848-271455 A) with dimensions of 40 $mm\times$ 40 $mm\times$ 4 mm, and operating temperature 150 $^\circ C$ and thermal conductivity of 0.015 $(W/m.K)$ was used as the energy harvester. An aluminum box with thin walls and 0.6 mm thickness, and total volume of 128 cm^3, and dimensions of 80 $mm\times$ 40 $mm\times$ 40 mm, was fabricated in order to store the PCM, and to place the copper and nickel foams. The thermoelectric system consisted of a 12 V DC fan (ZhangPeng 4010H) and an aluminum heat sink fabricated with dimensions of 16 $mm\times$ 40 $mm\times$ 40 mm and 5 fins each with a height and thickness of 15 mm and 4.4 mm, respectively, for cooling of the TEG module. K-type thermocouples with temperature measurement range up to 1250 $^\circ C$ and 0.75 % error were used to measure temperature of critical points in the system. The location of the thermocouples is also shown in Fig. 2A. As shown in Fig. 2B, the system was insulated using K-Flex insulator with thermal conductivity of 0.036 $(W/m.K)$ and average thickness of 25 mm to prevent heat loss from the system.

Table 1 presents the characteristics of the PCM used in this study. Features of the metal foams exerted in the tests are, furthermore, given in Table 2.

With the specifications of the system elements and Eqs. (1) and (2), the thermal resistance and heat capacitance of the heat storage module components from A to B (see the Fig. 1) before adding the foams are calculated in Table 3.

Therefore, $R_{th,AB}$ and $C_{th,AB}$ are calculated using Eqs. (5) and (6) as 4.56 (K/W) and 219.77 (J/K), while the PCM is in solid phase. For the liquid PCM, these values are 4.64 (K/W) and 145.02 (J/K), respectively. After combining the foams with the PCM inside the aluminum box and calculating thermal conductivity of the porous

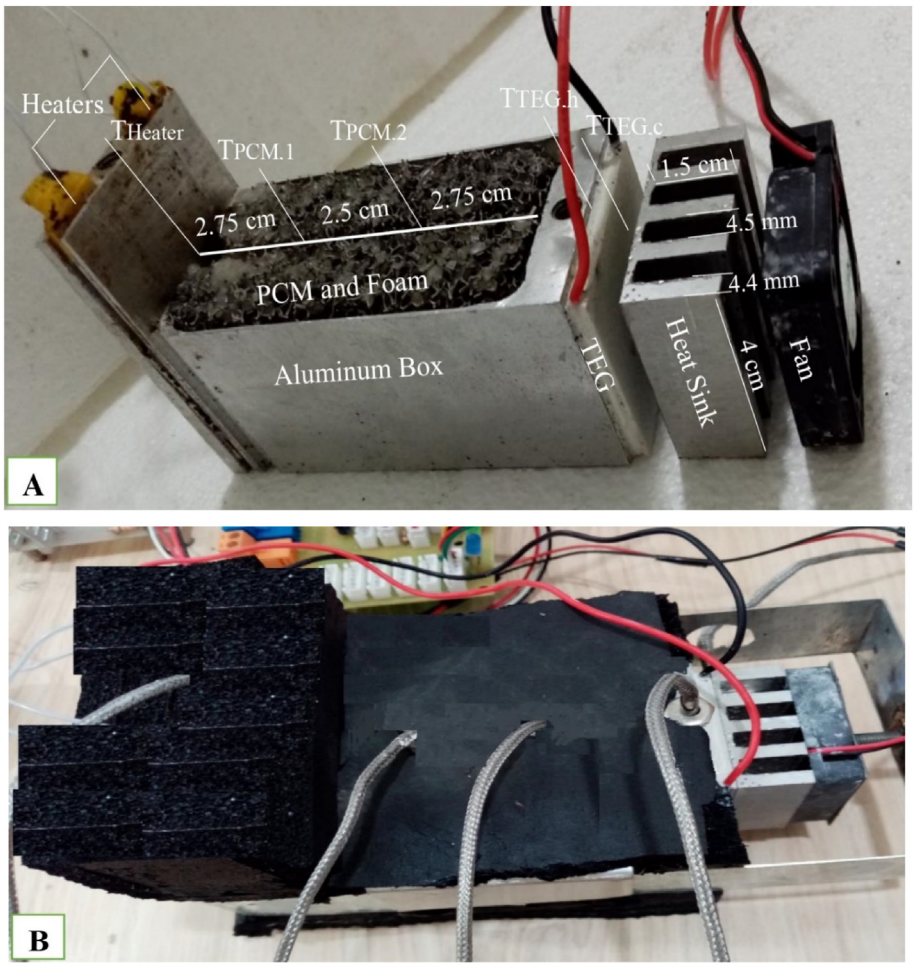

Fig. 2. A: The TEG system configuration and the location of the temperature sensors in the system. The depth of the sensors location inside the box is 2 cm. B: Insulated thermoelectric system.

Table 1
Properties of the phase change material [42].

PCM name	$T_m(^\circ C)$	$\rho(kg/m^3)$	$L(kJ/kg)$	$C_p(kJ/kg.K)$	$k_{th}\ (W/m.K)$
Paraffin wax	56	670 (s) 640 (l)	142.7	2.4 (s) 1.6 (l)	0.4 (s) 0.2 (l)

Table 2
Metal foams properties with dimensions of 4 cm × 4 cm × 8 cm and tolerance of.±0.1 mm.

Sample	*Pores per inch (PPI)*	*Porosity*	$C_p(kJ/kg.K)$	$\rho(kg/m^3)$	$k_{th}\ (W/m.K)$
Copper	20	0.90	0.385	8933	401
Nickel	20	0.90	0.440	8900	90.7

Table 3
Thermal resistance and heat capacitance of the components from A to B in Fig. 1 before adding metal foam.

material	*h* (mm)	*w* (mm)	*l* (mm)	*k* $(W/m.K)$	R_{th} (K/W)	ρ (kg/m^3)	C_{app} $(J/kg.K)$	C_{th} (J/K)
Al	80	0.6	120	235	4.73	2700	897	13.95
PCM (s)	80	40	40	0.4	125	670	2400	205.82
PCM (l)	*80*	40	40	0.2	250	640	1600	131.07

Table 4
Thermal resistance and heat capacitance of the porous medium in Fig. 1.

material	*h* (*mm*)	*w* (*mm*)	*l* (*mm*)	k_{eff} ($W/m.K$)	R_{pm} (K/W)	$\overline{\rho C}$ (kJ/m^3K)	$C_{th,pm}$ (J/K)
PCM (s) and copper	80	40	40	40.46	1.236	1791.12	229.26
PCM (l) and copper	80	40	40	40.28	1.241	1265.52	161.98
PCM (s) and nickel	80	40	40	9.43	5.30	1789.85	229.10
PCM (l) and nickel	80	40	40	9.25	5.40	1313.2	168.09

medium, k_{eff}, and $\overline{\rho C}$ with Eqs. (15) and (17), Table 4 is formed.

Using Eqs. (11) and (12), $R_{th,AB}$ and $C_{th,AB}$ are calculated with porous medium in the box, as shown in Table 5.

The results of theoretical calculations confirm the increment in the heat capacitance and reduction in the thermal resistance after addition the foams to the PCM, where the copper foam has led to a more reduction in the thermal resistance than the nickel.

4. Tests procedure

This section categorizes the experiments performed in this study. Three cases, namely PCM-only, PCM-Ni, and PCM-Cu were tested under both continuous and rectangular shape heat loads with different heat load frequencies. Electrical response of the TEG affected by heat transfer mechanism in the PCM box were compared for these three cases. The PCM box contained 128 cm^3 PCM in the PCM-only case and 115.2 cm^3 of the energy storage material in the cases comprising the metal foams. Porosity of the foams were $\varepsilon = 0.9$. In the experiments, the temperatures on the cold and hot sides of the TEG, inside of the PCM, the ambient and insulation as well as voltage output of the TEG were measured and recorded.

Although the internal resistance of the TEG is a function of temperature, its average value was determined to apply a fixed external load resistance in the experiments. When the TEG is under open circuit, minimum heat flux passes across the TEG. As the external load over the TEG decreases, higher heat is pumped across the TEG from its hot side to its cold side changing the thermal balance and temperature distribution on both sides of the module. When the internal and external resistances are equal, the output voltage is half of the open circuit voltage, and the power output is maximum [43]. With various electrical loads applied on the TEG circuit, external load resistance of 5 Ω, providing maximum power output, was selected and used in the experiments.

To investigate the melting process and effect of the foams on the phase change process, the system in the studied cases were heated with continuous heat fluxes, 5, 10, 15 and 20 W. The trend of the heat flux variation was used to analyze phase change performance of the PCM and heat transfer process in the system. To study the heat transfer mechanism in the system under fluctuation heat loads, rectangular heat loads of 10, 15, 20 and 25 W with intervals of 150, 300 and 600 s were applied. Table 6 shows the heat fluxes and considered applied times. For illustration, the continues heat load of 10 W and fluctuating heat load of 20 W applied on the system are shown in Fig. 3.

To ensure repetition of the experimental data, each test was performed three times. Standard deviation of the variables, the temperatures and output voltage, was calculated as follow [44]:

Table 6
Pattern of applied heat loads in the experiments.

Heat flux	Electric power (W)	Heater on (s)	Heater off (s)
constant	5, 10, 15, 20	1800	3600
step	10, 15, 20, 25	300	300
step	15	150	150
step	15	600	600

$$s_X = \left[\frac{1}{N-1}\sum_{i=1}^{N}(X_i - \overline{X})^2\right]^{\frac{1}{2}} \tag{28}$$

where N is number of the measurements. The mean value of X is defined as:

$$\overline{X} = \frac{1}{N}\sum_{i=1}^{N} X_i \tag{29}$$

The uncertainty of the hot and cold sides temperature and the output voltage in this study are calculated $\pm 1.5^{\circ}C$, $\pm 1^{\circ}C$ and 0.02 V, respectively.

5. Results and discussion

To have a comprehensive investigation on utilization of the metal foams under continues heat loads and at the ambient room temperature, the system's response during the melting and solidifying processes is evaluated. The fluctuating heat loads are used to study potential of energy storage in the PCM integrated with the transient power generation by the TEG. Various heat load periods can be a useful parameter to consider impact of the metal foams on the heat storage and heat transfer across the system. Using two metal foams with different thermal conductivities supports distinguishing the impact of metal foam material properties on the enhanced heat transfer rate and distribution in the storage box and electrical response of the TEG to the variations of the heat loads. Temperatures of the heat source, the PCM along the heat flow, hot and cold surfaces of the TEG, the insulation layer and ambient as well as voltage output of the TEG were recognized as the critical parameters to measure and assess thermo-electrical performance of the system.

Fig. 4 shows variation of the measured temperatures and voltage during the heating/cooling (on/off) stages in the system with PCM-only and continuous heating load of 20 W. Thermal conductivity of the PCM in the liquid phase is lower than that in the solid phase. Therefore, when the PCM reaches the melting point, heat transfer in the liquid PCM decreases as well as the heat

Table 5
$R_{th,AB}$ and $C_{th,AB}$ with porous medium in the box.

material	Copper foam and PCM (s)	Copper foam and PCM (l)	Nickel foam and PCM (s)	Nickel foam and PCM (l)
$R_{th,AB}(K/W)$	0.98	0.98	2.5	2.5
$C_{th,AB}(J/K)$	243.21	175.93	243.05	182.04

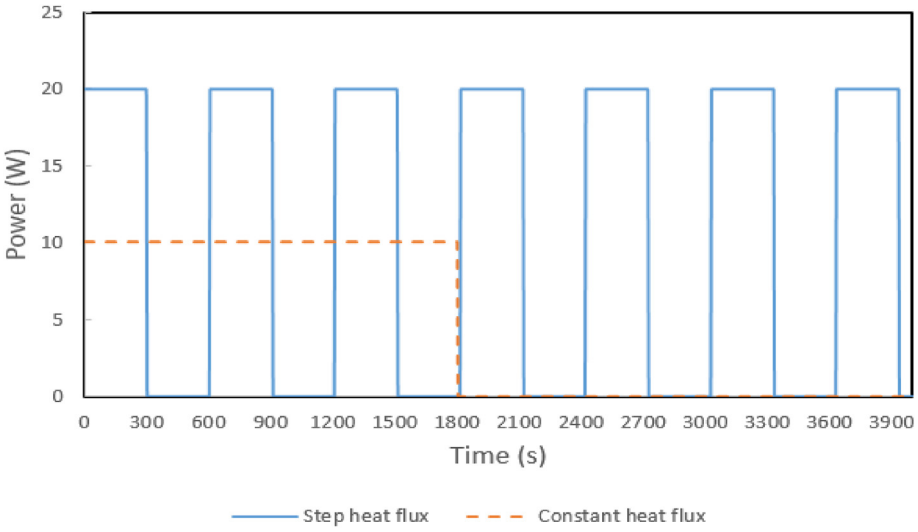

Fig. 3. Electrical power imposed by the heater for the continuous 10 W and fluctuating 20 W with intervals of 300 s.

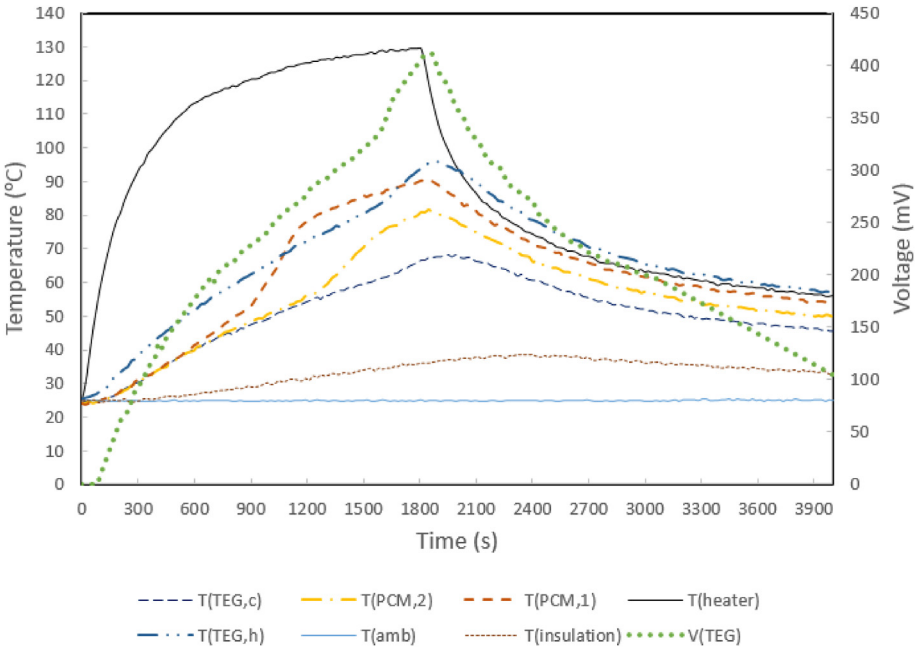

Fig. 4. The system with the PCM-only under continuous heat flux of 20 W.

transfer to the solid PCM at the middle of the box. Since the heat flux from the heat source is continues, increment rate of the temperature of the liquid phase becomes higher. Variation of the TEG's hot side temperature is a function of the thermal conductance between the heater and the TEG including the temperature and thermal conductivity of the PCM in both phases and thermal conductance of the box's walls. Hence, the temperature becomes higher than the PCM after the melting process due to the heat conductance across the walls. According to Eq. (23), the temperature difference across the TEG module provides the voltage output as shown in Fig. 4.

5.1. Thermal storage temperature

During the single heating stage, the PCM-only, PCM-Ni and PCM-Cu systems were exposed to continuous heat loads of 5, 10, 15 and 20 W staring from the room temperature and 1800 s. Fig. 5 shows the PCM temperature variation closer to the heat source at various studied heat loads. Due to high thermal conductivity, (see Eq. (15) and Table 4), the foams conduct the heat into the PCM during the heating process. According to the RC network shown in Fig. 1, the foams in the box add a parallel factor of thermal conductivity to the system RC network. Thus, the thermal resistance of the system decreases (see Table 5) and facilitates the heat transfer across the system. Because copper has a higher thermal conductivity and thermal diffusivity than nickel, the PCM temperature with the copper foam is higher than the case comprised nickel foam. After the heating stage, this process is reversed where the copper transfers heat from the PCM to the TEG with a higher rate. Thus, the temperature in the PCM-Cu box decreases quicker than the temperature in the PCM-Ni box.

For the systems under the 5 W heat load, the heater was turned

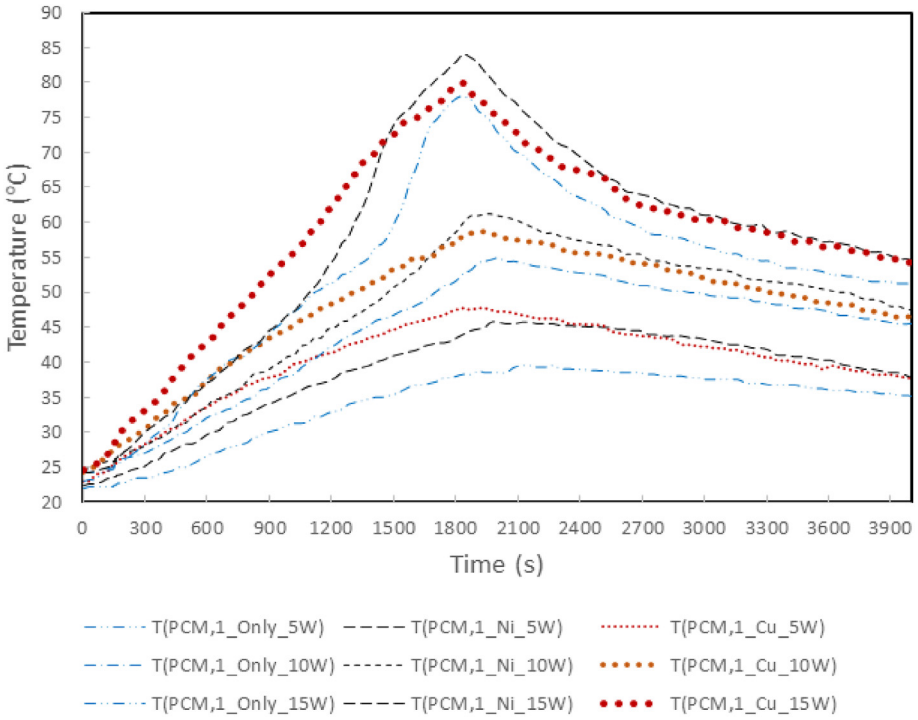

Fig. 5. Variation of PCM temperature close to the heater under in continuous heat flow of 5 W, 10 W, 15 W.

off before the melting process began. Therefore, higher heat loads were also applied to investigate the melting process of the PCM. With an input thermal power of 10 W, Fig. 5 shows that the melting process in the PCM-Cu started sooner than the case with PCM-Ni. Only at higher heat loads the melting process can be completed. Fig. 5 shows at heat load of 15 W the PCM melts in all the three cases, yet with different patterns. For instance, the melting pattern in the PCM-Cu is more uniform than the other cases, while the melting patterns of the PCM-only and PCM-Ni are similar. Because of the high thermal conductivity of the copper, heat transfer to the PCM happens with higher rate and phase change process occurs quicker. After the melting point, the PCM temperature with the copper foam becomes lower than the PCM temperature with the nickel foam because of the higher heat transferred to the PCM by the copper.

5.2. Hot and cold side temperatures of TEG

According to Eqs. (23) and (27), the hot and cold side temperatures of the TEG module have major impact on its output power. Fig. 6 shows impact of utilizing the metal foams on these temperatures. The higher thermal conductivity of the copper foam enhances heat storage rate and makes that the TEG taking less heat compared to the other cases. Therefore, the hot side temperature of the TEG before completion of the melting process is lower than that in the other systems. On the other hand, this material property of the copper conducts higher rate of the stored heat to the TEG after the heating stage and provides higher temperature at the hot side of the TEG.

5.3. Electrical power generation

Since the electrical load resistance was fixed at 5 Ω during the experiments, the temperature difference across the TEG was the most dominant factor in variation of the power generation by the TEG. Fig. 7 shows the power generation by the systems considered in this study. The cold side temperature of the TEG follows the temperature variation on the hot side. Therefore, the TEG's power generation in the studied systems are almost the same before the melting process. The higher heat conductance via the metal foams also improves the power generation after the heating process. As can be seen in Fig. 7, the copper foam is able to create higher temperature difference across the TEG and provides higher electrical power. The Maximum output power for the PCM-Cu case under 20 W heat flow was measured 13 mW. This value was 10.1 mW and 8 mW for the PCM-Ni and PCM-only systems, respectively. Therefore, the maximum power generated in the PCM-Cu and PCM-Ni systems increased by 62.5% and 26.2%, respectively, compared to the PCM-only system.

5.4. Heat source temperature

In this study, the electrical heater imposed the thermal energy into the PCM module. The heat source temperature, therefore, can be different at different heat loads and also for the different cases in this study. Fig. 8 shows the temperature variation of the heat source at 5 W and 10 W heat loads.

During the heating stage, the copper foam conducts a fraction of the thermal energy to the PCM more than the nickel. The lower thermal conductivity reduces the heat flux across the PCM and causes higher temperature at the heat source. For the case with PCM-only, with the lowest thermal conductivity, the heat source has the highest temperature. The results show that, application of the metal foams is an effective technique to protect and reduce temperature of the heat source in case of using low thermal conductivity PCMs in energy storage applications.

5.5. Fluctuating heat load

The heat imposed to an energy system may have variable

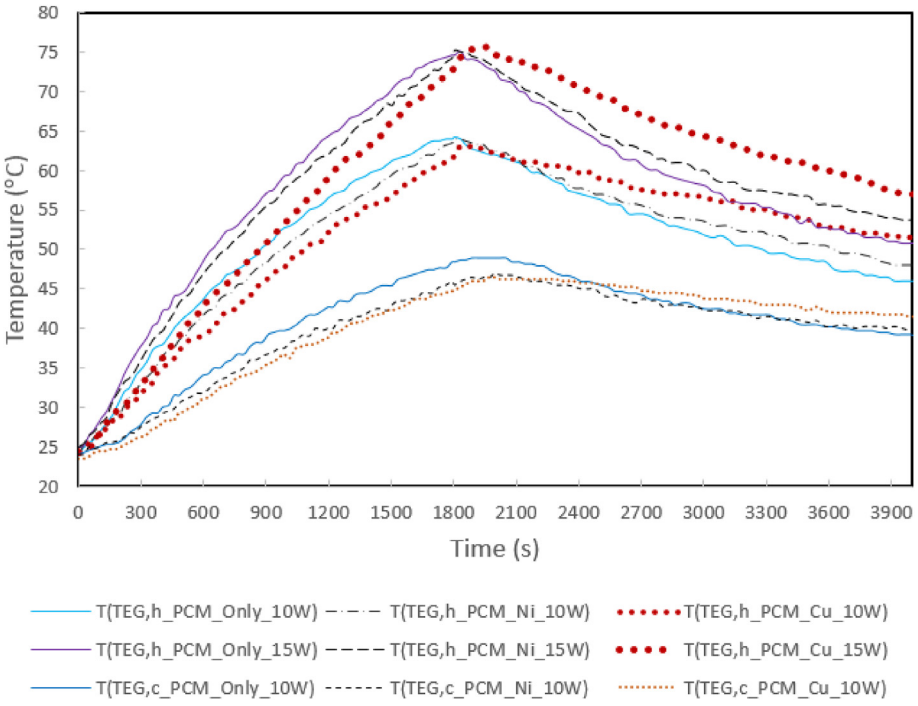

Fig. 6. The hot side temperature of the TEG module under 10 W, 15 W heat loads, and the cold side temperature under 10 W.

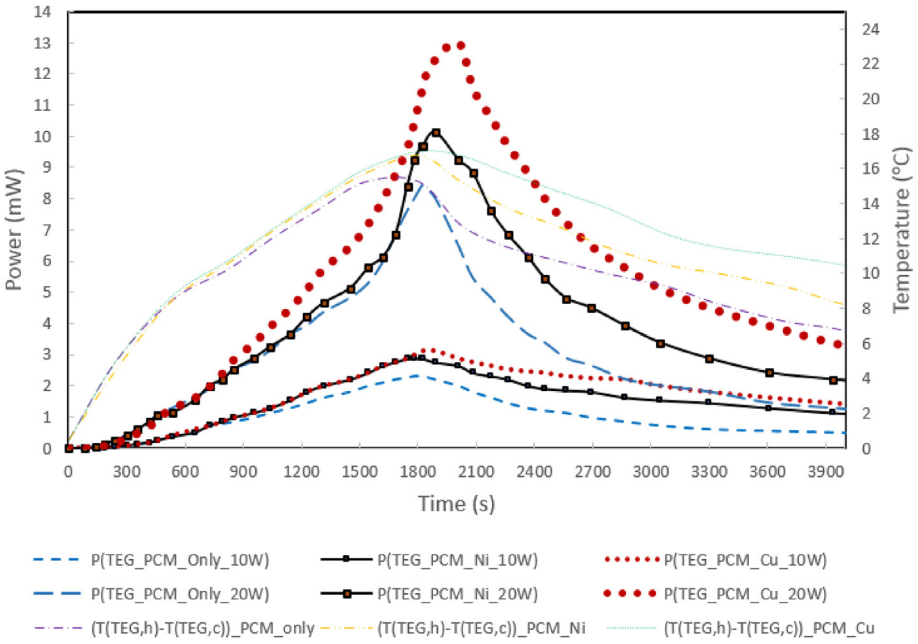

Fig. 7. Power generation under 10 W and 20 W, and temperature difference between the two sides of the module under 10 W.

properties. To expand performance evaluation of the energy storage systems over wider range of heat flows, various heat loads with different on/off time frequencies were applied to the hot side of the PCM box in the current study. Variation of the PCM temperature inside the box under 10 W and 25 W fluctuating heat loads is shown in Fig. 9.

The average melting point was 56 °C, thus it is clear that the copper and nickel foams accelerated the melting process time compared to the PCM-only case. Among the metal foams studied for reducing the thermal storage time, the copper foam provided best performance before the melting process was completed. However, at high heat loads the temperature of the PCM-Ni is slightly above the temperature of the PCM-Cu when the PCM is in the liquid phase. This is because the lower thermal conductance nickel foam transfers lower heat than the cooper to the cold side of the PCM module. Therefore, the PCM-Ni offers better performance for thermal energy storage in the box under long term step heating process. As shown in Fig. 9, long time requiring for transforming the PCM into liquid phase is noticeable under lower heat loads.

Prior and during the melting process the temperature drop of

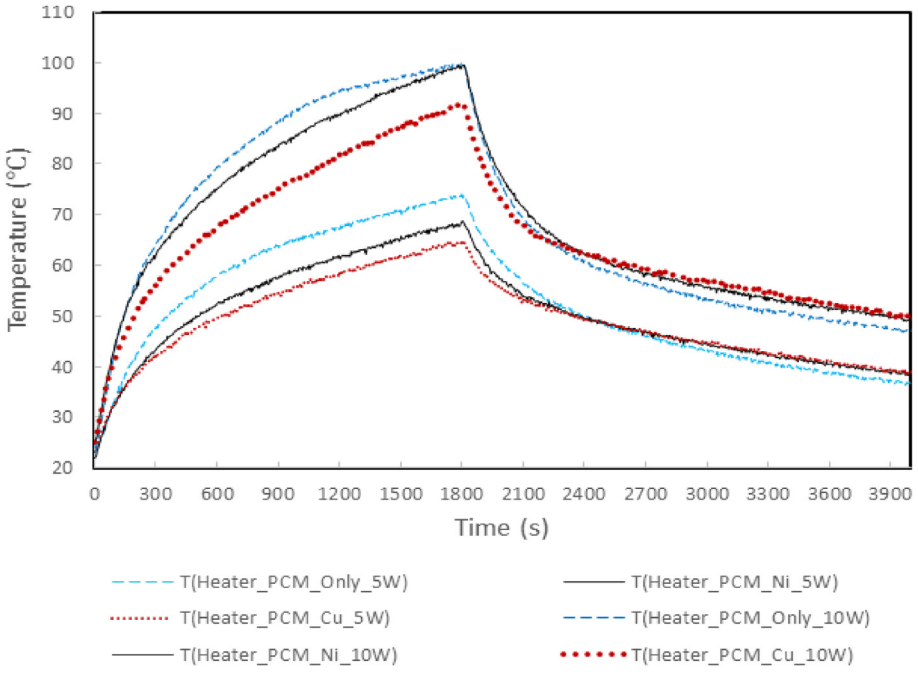

Fig. 8. The heat source temperature variation at continuous power of 5 W, 10 W.

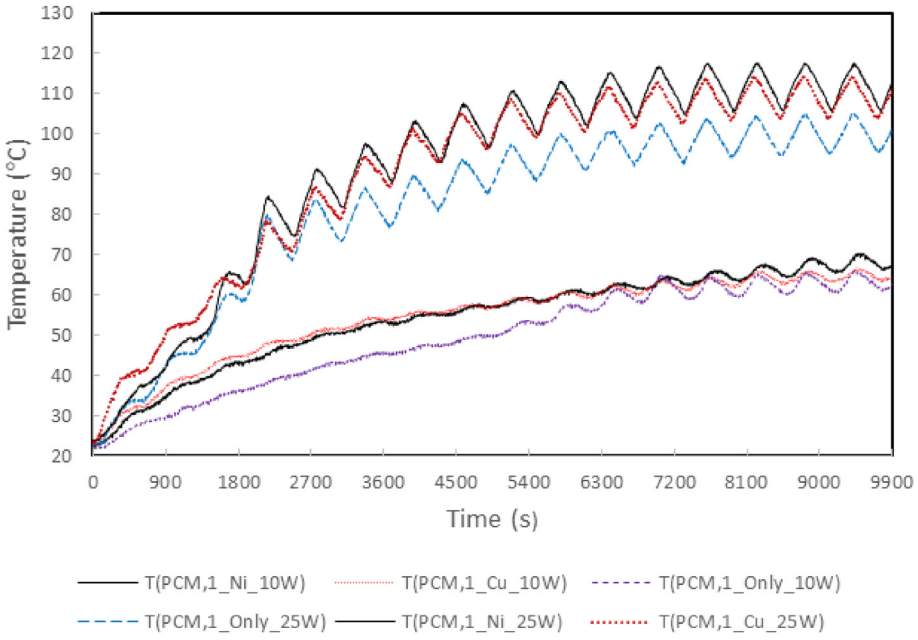

Fig. 9. Variation of PCM temperature ($T_{PCM,1}$) under 10 W and 25 W step heat flows with 300 s on/off time frequency.

the PCM was not significant when the heater was off. In this stage, the thermal potential between the foams, the box, and the PCM increased the PCM's temperature, and the thermal energy was storing in the PCM as latent heat. As the thermal conductivity and specific heat of the PCM is lower in the liquid phase compared to the solid phase (see Table 3), the PCM temperature is more affected by variation of the heat flow pattern and fluctuates radically. Fig. 10 shows that, for the longer on/off periods this variation is more significant. Because of similarity of the PCM temperature variation in the cases with PCM-Cu and PCM-Ni under fluctuating heat loads, the results for only PCM-Ni system are presented in this figure.

The effect of the metal foams, utilized in the PCM module, on the hot and cold side temperatures of the TEG and output power can be seen in Fig. 11 for sample fluctuating heat load of 20 W.

Because the PCM temperature inside the box is higher during the melting process, due to the higher thermal storage rate, the temperatures of the TEG are lower for cases comprising the metal foams. It is noteworthy that, after the melting process the hot side temperature of the TEG is higher because thermal energy discharging in the PCM occurs with higher rate due to the higher thermal conductivity of the metal foams. Utilization of the metal foams under the fluctuating loads provides higher power

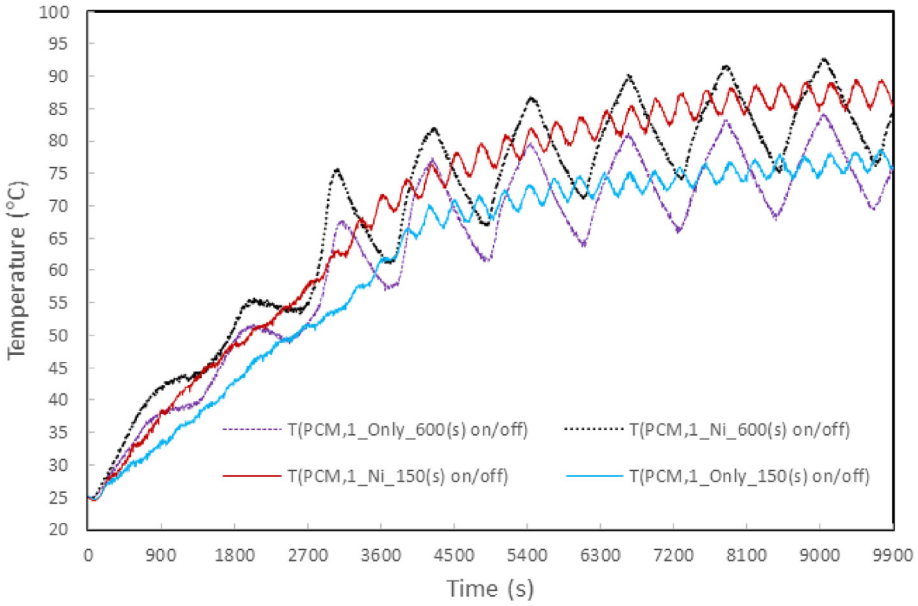

Fig. 10. Variation of the PCM temperature ($T_{PCM,1}$) in step heat flow 15 W, 150 s and 600 s on/off.

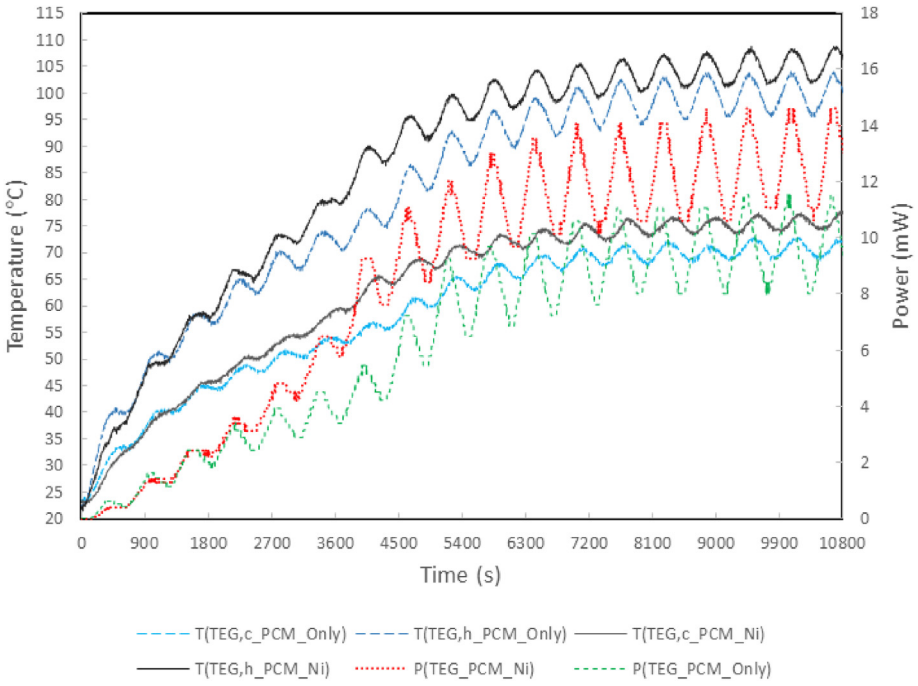

Fig. 11. Temperature variation on the hot and cold sides of the TEG and Power generation under step load of 20 W, 300 s on/off.

generation after the melting process because of making the greater temperature difference across the TEG module. The maximum power generation in the PCM-Ni and PCM-only systems was 14.6 *mW* and 11.5 *mW*, respectively. Therefore, the power generation in the system including the metal foam increased up to 26.9% compared to the PCM-only system.

The results show that, porous metal foams have a significant effect on increasing overall thermal conductivity of the PCM module and heat transfer rate between the heat source and the TEG. Therefore, applying thermally conductive metal foams can improve economic savings in energy production systems under fluctuating heat sources. Such heat sources can be found in power electronics systems, radiative heat transfer systems in windy environments [45], and renewable energy systems [46]. Moreover, automotive industry, environmental sensors [37], and heat recovery systems integrated with protective system from overheating can be other applications of such advancement. Temperature control on both sides of a TEG and protection of the module from overheating are critical challenges in systems operating under unstable thermal boundary conditions, and the combination of PCM and porous metal foams can offer a sustainable solution for these challenges.

6. Conclusions

In this experimental study, effect of porous metal foams on heat transfer and thermal storage in a PCM module was studied under transient thermal boundary conditions. The heat storage module was integrated with a TEG to explore impact of copper and nickel foams on enhancement of heat storage rate and electrical power generation in the hybrid PCM-TEG system particularly under transient heat loads. Therefore, temperature variation of the heat source, in the storage box, on the cold and hot sides of the TEG as well as voltage output of the TEG were measured under continuous heat loads imposed at ambient temperature and under fluctuating heat loads with various intervals.

Results of this study shows that, enhancement of overall thermal conductivity of the thermal storage module, due to the metal foams, is a key factor of heat transfer mechanism in the storage module and temperature of the TEG. In this study the copper foam provided higher thermal storage in the solid phase and during the melting process, while the nickel foam enhanced energy storage when the PCM was in its liquid phase. Overall, the copper foam provided higher electrical power over entire heating and cooling stages under the applied transient heat loads. The acceleration of heat transfer rate from the heat source to the TEG by the copper and nickel porous foams increased the power output of the TEG 62.5% and 26.2%, respectively, compared to the hybrid PCM-TEG system with PCM-only. The results of this study provide a guideline for enhancing heat transfer in thermal storage systems with PCMs by applying thermally conductive metal forms to improve economic savings in energy production systems under fluctuating heat sources.

Credit author statement

Esmaeil Yousefi: Writing- Original draft preparation, Experimental setup, Experimental data, Visualization. **Ali Abbas Nejad**: Methodology, Supervision, Investigation. **Alireza Rezania**: Conceptualization, Design of experiment, Methodology, Editing-Original draft preparation, Investigation, Supervision.

Declaration of competing interest

The authors declare that they have no known competing financial interests or personal relationships that could have appeared to influence the work reported in this paper.

References

[1] He W, et al. Recent development and application of thermoelectric generator and cooler. Appl Energy 2015;143:1–25.
[2] Luo D, Sun Z, Wang R. Performance investigation of a thermoelectric generator system applied in automobile exhaust waste heat recovery. Energy 2022;238:121816.
[3] Musharavati F, et al. Thermodynamic modeling and comparative analysis of a compressed air energy storage system boosted with thermoelectric unit. J Energy Storage 2021;33:101888.
[4] Ge M, et al. Structural optimization of thermoelectric modules in a concentration photovoltaic–thermoelectric hybrid system. Energy 2022:123202.
[5] Luo D, et al. Modelling and simulation study of a converging thermoelectric generator for engine waste heat recovery. Appl Therm Eng 2019;153:837–47.
[6] Yu J, et al. Analysis of temperature control effect of composite phase change structure used in thermoelectric conversion system. Appl Therm Eng 2020;167:114760.
[7] Rezania A, Rosendahl L. Evaluating thermoelectric power generation device performance using a rectangular microchannel heat sink. J Electron Mater 2011;40(5):481–8.
[8] Rezania A, Rosendahl L. New configurations of micro plate-fin heat sink to reduce coolant pumping power. J Electron Mater 2012;41(6):1298–304.
[9] Mohammadnia A, et al. Utilizing thermoelectric generator as cavity temperature controller for temperature management in dish-Stirling engine. Appl Therm Eng 2020;165:114568.
[10] Mohammadnia A, et al. Fan operating condition effect on performance of self-cooling thermoelectric generator system. Energy 2021;224:120177.
[11] Abbasi HR, Pourrahmani H. Multi-objective optimization and exergoeconomic analysis of a continuous solar-driven system with PCM for power, cooling and freshwater production. Energy Convers Manag 2020;211:112761.
[12] Demirkıran İG, Cetkin E. Emergence of rectangular shell shape in thermal energy storage applications: fitting melted phase changing material in a fixed space. J Energy Storage 2021;37:102455.
[13] Motiei P, Yaghoubi M, GoshtasbiRad E. Transient simulation of a hybrid photovoltaic-thermoelectric system using a phase change material. Sustain Energy Technol Assessments 2019;34:200–13.
[14] Lee G, et al. Flexible heatsink based on a phase-change material for a wearable thermoelectric generator. Energy 2019;179:12–8.
[15] Meng J-H, et al. Heat transfer mechanism and structure design of phase change materials to improve thermoelectric device performance. Energy 2022;245:123332.
[16] Wang J, et al. Experimental investigation on the influence of phase change material on the output performance of thermoelectric generator. Renewable Energy; 2021.
[17] Altstedde MK, Rinderknecht F, Friedrich H. Integrating phase-change materials into automotive thermoelectric generators. J Electron Mater 2014;43(6):2134–40.
[18] Jaworski M, Bednarczyk M, Czachor M. Experimental investigation of thermoelectric generator (TEG) with PCM module. Appl Therm Eng 2016;96:527–33.
[19] Atouei SA, Ranjbar AA, Rezania A. Experimental investigation of two-stage thermoelectric generator system integrated with phase change materials. Appl Energy 2017;208:332–43.
[20] Atouei SA, et al. Protection and thermal management of thermoelectric generator system using phase change materials: an experimental investigation. Energy 2018;156:311–8.
[21] Darkwa J, et al. A numerical and experimental analysis of an integrated TEG-PCM power enhancement system for photovoltaic cells. Appl Energy 2019;248:688–701.
[22] Yu J, et al. A novel structure for heat transfer enhancement in phase change composite: rolled graphene film embedded in graphene foam. ACS Appl Energy Mater 2019;2(2):1192–8.
[23] Li H, et al. Visualized-experimental investigation on the energy storage performance of PCM infiltrated in the metal foam with varying pore densities. Energy 2021;237:121540.
[24] Radomska E, Mika L, Sztekler K. The impact of additives on the main properties of phase change materials. Energies 2020;13(12):3064.
[25] Senobar H, Aramesh M, Shabani B. Nanoparticles and metal foams for heat transfer enhancement of phase change materials: a comparative experimental study. J Energy Storage 2020;32:101911.
[26] Bose JR, et al. Comprehensive case study on heat transfer enhancement using micro pore metal foams: from solar collectors to thermo electric generator applications. Case Stud Therm Eng 2021;27:101333.
[27] Chen X, et al. Thermal storage analysis of a foam-filled PCM heat exchanger subjected to fluctuating flow conditions. Energy 2021;216:119259.
[28] Borhani S, et al. Performance enhancement of a thermoelectric harvester with a PCM/Metal foam composite. Renew Energy 2021;168:1122–40.
[29] Duan J. A novel heat sink for cooling concentrator photovoltaic system using PCM-porous system. Appl Therm Eng 2021;186:116522.
[30] Nithyanandam K, Mahajan R. Evaluation of metal foam based thermoelectric generators for automobile waste heat recovery. Int J Heat Mass Tran 2018;122:877–83.
[31] Madruga S. Thermoelectric energy harvesting in aircraft with porous phase change materials. In: IOP Conference Series: Earth and environmental Science. IOP Publishing; 2019.
[32] Diani A, Campanale M. Transient melting of paraffin waxes embedded in aluminum foams: experimental results and modeling. Int J Therm Sci 2019;144:119–28.
[33] Li W, et al. Experimental investigation on combined thermal energy storage and thermoelectric system by using foam/PCM composite. Energy Convers Manag 2021;243:114429.
[34] Tuoi TTK, Van Toan N, Ono T. Theoretical and experimental investigation of a thermoelectric generator (TEG) integrated with a phase change material (PCM) for harvesting energy from ambient temperature changes. Energy Rep 2020;6:2022–9.
[35] Stupar A, Drofenik U, Kolar JW. Optimization of phase change material heat sinks for low duty cycle high peak load power supplies. IEEE Trans Compon Packag Manuf Technol 2011;2(1):102–15.
[36] Tiari S, Mahdavi M. Computational study of a latent heat thermal energy storage system enhanced by highly conductive metal foams and heat pipes. J Therm Anal Calorim 2020;141(5):1741–51.
[37] Madruga S. Modeling of enhanced micro-energy harvesting of thermal ambient fluctuations with metallic foams embedded in Phase Change Materials. Renew Energy 2021;168:424–37.
[38] Mahdi JM, et al. Solidification enhancement with multiple PCMs, cascaded metal foam and nanoparticles in the shell-and-tube energy storage system. Appl Energy 2020;257:113993.
[39] Ming T, et al. Analytical and numerical investigation on a new compact thermoelectric generator. Energy Convers Manag 2017;132:261–71.
[40] Weera S, Lee H, Attar A. Utilizing effective material properties to validate the

performance of thermoelectric cooler and generator modules. Energy Convers Manag 2020;205:112427.
[41] Rezania A, Yazdanshenas E. Effect of substrate layers on thermo-electric performance under transient heat loads. Energy Convers Manag 2020;219:113068.
[42] Murali G, Mayilsamy K, V Arjunanc T. An experimental study of PCM-incorporated thermosyphon solar water heating system. Int J Green Energy 2015;12:978–86.
[43] Chen W-H, et al. A computational fluid dynamics (CFD) approach of thermoelectric generator (TEG) for power generation. Appl Therm Eng 2020;173:115203.
[44] Coleman HW, Steele WG. Experimentation, validation, and uncertainty analysis for engineers. John Wiley & Sons; 2018.
[45] Mirhosseini T, et al. Harvesting waste heat from cement kiln shell by thermoelectric system. Energy 2019;168:358–69.
[46] Mahmoudinezhad S, et al. Response of thermoelectric generators to Bi2Te3 and Zn4Sb3 energy harvester materials under variant solar radiation. Renew Energy 2020;146:2488–98.